

A Distributed Data Store in Orbit

Jörg Ott Technical University of Munich Germany Jussi Kangarharju University of Helsinki Finland Nitinder Mohan
Delft University of Technology
Netherlands

ABSTRACT

Emerging Low Earth Orbit (LEO) satellite constellations have been considered for uses beyond plain Internet access, including content caching and edge computing. Assuming satellites are equipped with inter-satellite links, we propose using these links and thus the space in-between satellites, paired with a dedicated satellite queuing system, to "store" data and provide access by keeping data in constant flux around the globe. We describe the properties and explore the capabilities of such a system and discuss some potential uses.

CCS CONCEPTS

 Networks → Network architectures; Network protocol design; Network simulations.

KEYWORDS

Low Earth Orbit Satellite Systems; Distributed Storage

ACM Reference Format:

Jörg Ott, Jussi Kangarharju, and Nitinder Mohan. 2025. A Distributed Data Store in Orbit. In 3rd Workshop on LEO Networking and Communication (LEO-Net '25), September 8–11, 2025, Coimbra, Portugal. ACM, New York, NY, USA, 10 pages. https://doi.org/10.1145/3748749.3749093

1 INTRODUCTION

As Low-Earth Orbit (LEO) satellite megaconstellations extend the reach of the Internet, speculations about further use beyond plain Internet access arise. These include ideas about caching content in space [7, 13], CDNs [4], computation in orbit [2, 11], edge computing in space [5, 8], and application-specific data aggregration, e.g., in the context of scientific data sensing from space [5]. Building satellite-based content delivery systems would usually require some control plane to locate content objects, route requests, perform load balancing, etc. and possibly actively manage content caches [4].

In this paper, we take a different route: we continuously move content objects, represented as a series of packets, around in the orbital shell, i.e., across all satellites on all orbits at the same altitude of a megaconstellation, one orbit at a time, so that satellites can just wait for objects, eliminating the need for active discovery. We leverage the large distances in space and the high data rate of intersatellite laser links, which together yield a substantial bandwidth-delay-product, to "store" content as *data in flight* between satellites in addition to providing extra storage on each satellite. In a sample configuration (see fig. 3 and 4), a single content object would traverse

Permission to make digital or hard copies of all or part of this work for personal or classroom use is granted without fee provided that copies are not made or distributed for profit or commercial advantage and that copies bear this notice and the full citation on the first page. Copyrights for third-party components of this work must be honored. For all other uses, contact the owner/author(s).

LEO-Net '25, September 8–11, 2025, Coimbra, Portugal © 2025 Copyright held by the owner/author(s). ACM ISBN 979-8-4007-2090-1/25/09 https://doi.org/10.1145/3748749.3749093

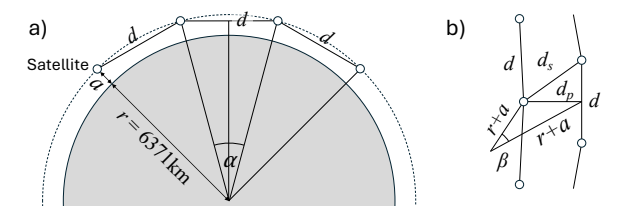


Figure 1: a) Distance d between two satellite in the same orbit and b) d_s between the two closest satellites in adjacent orbital planes.

all 1,584 satellites (22 in each of 72 orbits) of the lowest Starlink orbital shell at 550 km altitude approximately every 11 seconds, covering a total distance of 3.27M kilometers.

We present our assumptions and system model in §2 along with the resulting basic system properties, especially the tradeoffs between storage capacity, content replication, and access latency. We discuss mechanisms for adding, replicating, deleting, and routing content objects in §3 and show via simulations how far simple local algorithms with limited state and a lightweight protocol can carry in §4. We conclude with a sample usages and a discussion of possible directions in §5.

2 DESIGN

We assume a LEO satellite constellation in a single orbital shell that covers the inhabited Earth surface with sufficient satellite density that each point on the ground within the coverage area is served by at least one satellite at any given instant. Each LEO satellite is equipped with four lasers to establish ISLs at data rates of $R_{ISL}=100~{\rm Gbps}$. Two of the ISLs connect each satellite to its preceding and succeeding neighbors in the same orbital plane, the remaining two connect to satellites in adjacent orbits, creating a +grid topology [3]. We assume that the satellites have sufficient power to operate their ISLs continuously, which appears reasonable as current LEO deployments use ISLs. We only consider the operation of a single orbital shell but our considerations can be extended to multiple shells.

Each user terminal connects to exactly one satellite at a time. The terminal reaches the Internet via a bent pipe to a ground station and point of presence (PoP) of the satellite operator. We assume that Internet traffic is routed to the closest ground station and does not traverse many ISLs, minimizing ISL use by end user traffic, so that the satellite operator may bound end user ISL traffic and dedicate an ISL capacity share to *storage traffic* f_s .

Satellites of an orbital shell O are at an altitude a and at an inclination γ_o . The shell is comprised of N_p orbital planes with N_o satellites per orbital plane (or: orbit), assumed to be evenly spaced at an angular distance of $\alpha = 360^\circ/N_o$. With a mean Earth radius of r = 6371 km, this yields a distance (line of sight) of $d = 2(r+a)\sin(\frac{1}{2}\alpha)$ as shown in figure 1a. The distance between satellites

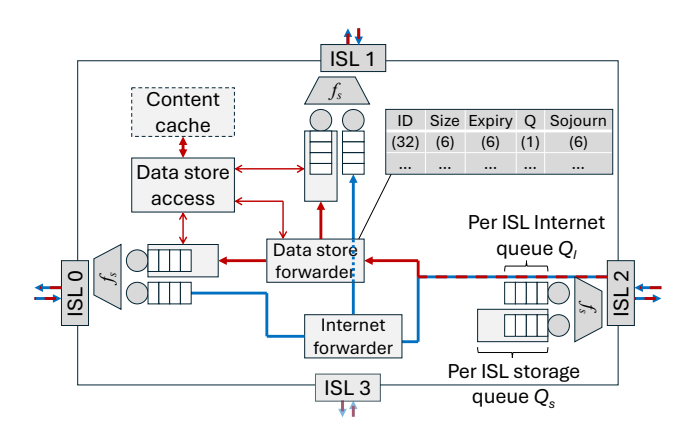


Figure 2: Satellite architecture showing three ISLs with their outbound queues for Internet and storage traffic and the respective forwarding logic, content object state table, and an incoming flow from ISL 2. A data access module matches incoming requests (not shown) against stored content objects with an optional cache.

on adjacent orbital planes varies, being largest at the equator. Figure 1b illustrates the maximum distance d_s between the closest satellites on neighboring planes: the planes are spaced an equal angles of $\beta=360^\circ/N_p$, yielding a distance of $d_p=2(r+a)sin(\frac{1}{2}\beta)$ (at the equator), and the satellites are at a maximum phase shift relative to each other, i.e., at an offset of $\frac{d}{2}$ within their respective orbits. The resulting maximum distance at the equator is then $d_s\approx\sqrt{\frac{1}{4}d^2+d_p}$. To reduce the system dynamics to be accounted for and to obtain a conservative estimate, we assume the maximum distance d_s for computing the propation delay and we ignore that storage capacity of the links across planes.

Consider the Starlink orbital shell at $a=550\,\mathrm{km}$ altitude with $N_p=72$ orbital planes at an inclination of $\gamma_0=53^\circ$ and $N_0=22$ satellites per orbit. The satellites on an orbital plane are spaced $d=1969.72\,\mathrm{km}$ apart, at the equator, the distance between two adjacent orbital planes is $d_p=603.78\,\mathrm{km}$, and the max distance between the closest satellites on neighboring orbital planes is $d_s=1155.29\,\mathrm{km}$.

2.1 System model

Figure 2 sketches part of a single satellite system focusing on the ISLs, i.e., not including the radio links to the ground stations and terminals. Each satellite, at a minimum, provides two send queues of different sizes per interface: one for regular (= Internet) traffic of size Q_I and one for storage traffic of size Q_S . The queues receive proportional treatment when scheduling packets for transmission on an ISL with a share f_S reserved for storage traffic, e.g., using weighted fair queuing.

A content object maintained in the data store comprises a sequence of packets, each packet including at least the content id (e.g., a hash) and total size, its data offset into the object, its expiration time, the total number of replicas and the replica instance number, and a (cryptographic) checksum. A meta data table on the satellite records per content object the id (32 bytes), size (6 bytes), expiration

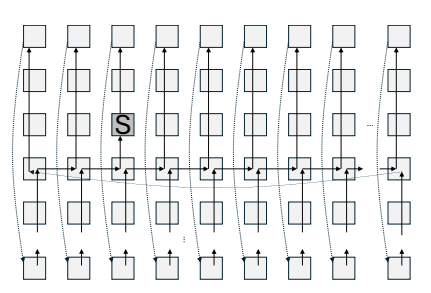


Figure 3: Simple propagation pattern of a single data object from its originator (S) first along each orbital plane and then in a defined area to the next plane.

time (6 bytes), sojourn time (6 bytes), and the storage queue (Q, 1 byte), plus internal maintence data, yielding some 64 bytes per record, so that 1M entries would only consume \approx 60 MB of memory.

The figure also shows packets incoming from ISL 2 that are classified into Internet and data store traffic and then handled by independent forwarding units that determine their respective next hops, e.g., ISL 0 or 1: the Internet forwarder implements regular L2 switching or IP routing while the data store forwarding logic comprises algorithms to ensure that content object packets circle through all satellites of an orbital shell, to insert, possibly replicate, and delete packets, and to perform error control. We will return such algorithm in §3 and assume for now that a simple one exists that forwards each packet along one orbit at a time and then shifts to the next plane, as illustrated in figure 3.

The data store access unit interfaces to all storage queues and responds to content object requests from satellite terminals (not shown). The data store forwarder records which content objects are in which ISL storage queue along with its expected sojourn time. Given sufficient capacity, a record could be kept for all objects in orbit until they expire and hold the # replicas per object (cf. §2.2) and when it last passed through this satellite. This tells the data store access unit from which queue to fetch the content object, whether it would be feasible to retrieve it from a nearby satellite, or to predict when when its next pass through this satellite is expected.

Content requests would, by default, arrive via the radio interfaces to the ground, but they could also be forwarded by neighbors if those cannot satisfy a request immediately or in the near future. We leave this cooperative caching-style optimization using known techniques for future work.

2.2 Basic properties and trade-offs

We now take a brief look at the theoretical properties of our design. With content objects in constant flux around the globe, two performance metrics are of particular interest: the total *storage capacity*, C_o , of the orbital shell and the *content periodicity*, t_a . The periodicity t_a is defined as the time elapsing between a given content object (or one of its replicas) passing twice through the same satellite and serves as a rough approximation of the worst case access latency from a terminal connected to that satellite.

For storage capacity, we consider: 1) the storage queue for each ISL transmitter, Q_S , and 2) the data in flight on each ISL, $F_S = \frac{d}{c} \times f_S \times R_{ISL}$, as per the link's bandwidth-delay product for the

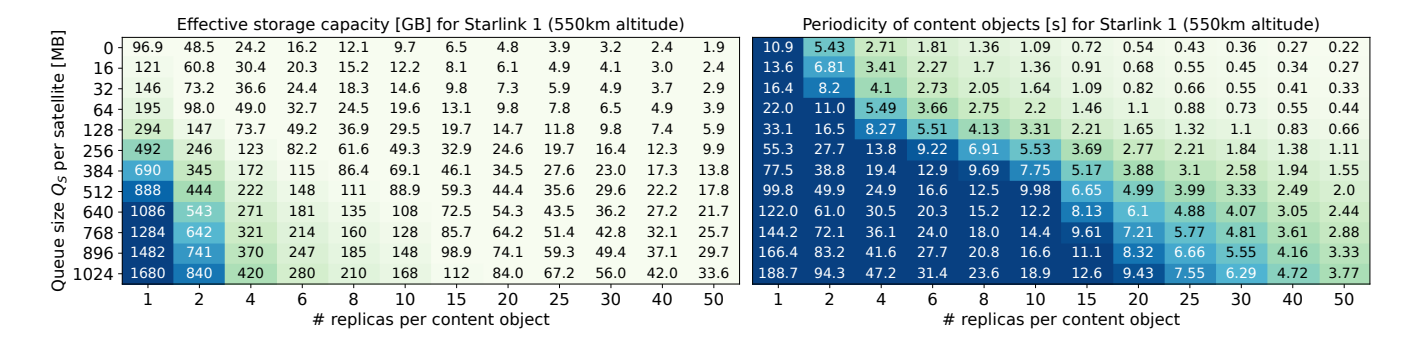


Figure 4: Effective storage space and periodicity of a content object passing through the same satellite as a function of the number of replicas and the content queue size per satellite for Starlink orbital shell at 550km altitude.

traffic share f_s , with c = 299,792.458 km/s. This yields a capacity per satellite (including one outgoing ISL within its orbit) of C_s = $Q_S + F_S$, per orbital plane of $C_p = C_S \times N_o$, and per orbital shell of $C_o = C_D \times N_D$. Due to their potential variability, we do not account for the capacity added by links across orbital planes. If K replicas of content objects are kept, the effective storage capacity of the shell is $C_e = \frac{C_o}{K}$.

For the latter, access latency, we compute how long it takes a single content item to pass through the entire orbital shell, t_0 . We consider the processing and queuing delays per satellite, t_f and t_q , respectively, as well as the propagation delay for each link within an orbital plane, t_p , and across orbital planes t_s . We assume $t_f = 0.1 \,\mathrm{ms}$ for each content object, which roughly matches the interarrival time of 1 MB sized objects at $R_{ISL} \times f_s = 80$ Gbps and allows for sufficient local processing and state management. We obtain the maximum $t_q = \frac{\hat{f}_s \times Q_S}{R_{ISL}}$ and the propagation delays as $t_p = \frac{d}{c}$ and the worst case $t_s = \frac{d_s}{c}$. This yields the maximum time for a content object to pass through all satellites of a shell, the rotation time, t_0 , as

$$t_o = N_o \times (t_f + t_q + t_p) + N_p \times (t_f + t_q + t_s)$$

for the above simple propagation pattern (fig. 3). As for storage capacity, we may assume K replicas of a content item evently spaced across all satellites, which would reduce the periodicity, i.e., the effective access latency to $t_a = \frac{t_o}{K}$.

Figure 4 shows the effective storage capacity C_o (left) and effective periodicity t_a (\approx access latency, right) for the Starlink orbital shell 1 at 550 km altitude. Assuming a target access latency of <10 s, we see that up to 20 replicas would be needed, whereas staying below 30 s 1-8 replicas suffice.

There is an obvious tradeoff between capacity and periodicity. Combining both, we may set a target periodicity and derive the necessary number of replicas for a given storage queue size, from which we can then compute the effective storage capacity. Doing this for all megaconstellations as per table 2 in Appendix B, we show the effective capacity of the data store for a target periodicity of 10 s as a function of the queue size in figure 5 (top). We find that increasing the storage queue size yields an increasing capacity, albeit not monotonically. The capacity growth is expectedly more pronounced for shells with fewer orbits (Starlink 3, 4, 5 use just 8, 5, and 6 orbits, respectively) as less data is "in flight" between satellites on fewer orbits. Fluctuation appears stronger for those

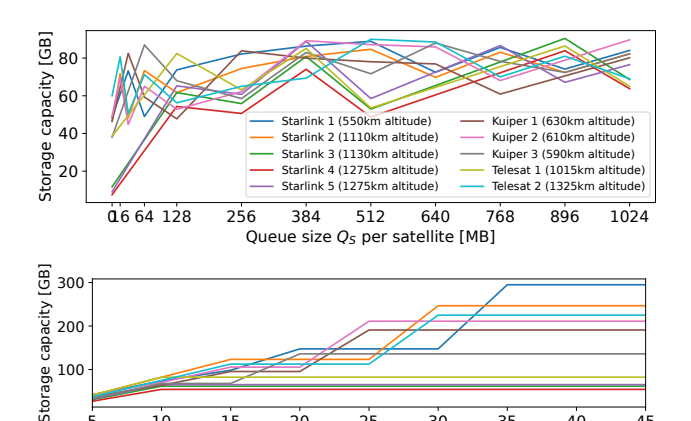


Figure 5: Storage capacity for the orbital shells of different megaconstellations for a target periodicity of 10 s (top) and for varying periodicity at 128 MB queue size (bottom)

Target periodicity [s]

35

40

45

shells with fewer satellites. As increasing queue capacity leads to longer object rotation times t_o , this needs to be compensated by additional replicas so that we observe dimishing (if any) returns. The capacity grows roughly linearly as a step function with increasing periodicity (figure 5, bottom). Overall, we obtain some 40-80 GB storage capacity for a periodicity of 10 s pretty much independent of the megaconstellation.

Above, we assume sending the content objects into one direction through the orbital plane, hence only considering half the available transmission and storage capacity. Using both directions would thus duplicate the available capacity and further reduce the latency; however, the intervals at which content objects pass through a satellite would no longer be uniformly distributed; this is left for future study.

OPERATION

10

15

20

So far for some theory. We now introduce a strawman algorithm to realize a baseline for storage in space, with routing (§3.1), inserting/deleting content (§3.2), and error handling (§3.3). We assume a system without malicious nodes which appears reasonable for closed satellite systems as today's megaconstellations are.

3.1 Steady state operation

A simple strawman routing algorithm as alluded to above makes a content object traverse one orbital plane and then, upon reaching the satellite it started at, move to the next orbital plane, shown in figure 6. We number the ISL interfaces clockwise as in figure 2; the odd numbered ones are for the North-South directions to satellites within the same orbit, the even numbered ones for East-Wast across orbits.

We assume that each storage packet carries two "hop" counters: n to indicate the count of the satellite in the present orbit and p to count the orbital plane: n allows determining when all satellites of a given orbital plane were visited, p determines when the entire orbital shell is covered. n is incremented whenever a packet is received from a satellite within the same orbital plane. If n reaches N_0 , n is reset to 0 and the packet is passed on to the next plane, incrementing p; otherwise, the packet is passed on to the next satellite within the same plane (cf. fig. 3). This works in either North-South direction.

```
Input: Packet pkt, Incoming interface # if_in
Return: Outgoing interface #
incomding_storage_pkt (pkt, if_in) {
    if (if_in %2 == 1) {
        // packets coming from a different orbital plane
        if (++pkt.p == N_p)
            pkt.p = 0;
        return (if_in + 1) % 4;
    }
    // packets coming from within the orbital plane
    if ((++pkt.n) == N_o) {
        pkt.n = 0;
        return (if_in + 3) % 4;
    else
        return (if_in + 2) % 4;
}
```

Figure 6: Simple routing algorithm to make a content object pass through all satellites of an orbital shell.

Over time, the algorithm needs to adjust n to ensure that a packet is always passed to a neighboring orbital plane when the sending satellite is close to the equator. This is easily achieved as the satellite can observe its own position and update n by ± 1 to pre- or postpone switching orbital planes.

Obviously, other (smarter) algorithms are conceivable within the limitations of the time-varying network topology. The task that each content item should traverse each satellite within the orbital shell translates into the well-known traveling salesman problem applied to a grid-like topology with recurring visits. Interesting questions could be how to use multiple salespersons (i.e., object replicas) to optimize the distribution of the time between repeated visits by the same or different salespersons for a given (non-)uniform utility function.

3.2 Adding and removing content

To add a content object into the distributed data store, the originating satellite defines the object metadata: id I, expiration time t_{ttl} , and replication factor R. The id I could be a cryptographic identifier of the creator plus a hash to identify the content, e.g., like a CID in IPFS [1]. Transmission of the replicas is evenly spaced by observing the current rotation time t_o of a single object, i.e., the time it takes the object to pass through all satellites of the orbital shell, and dividing this by R; each replica is associated with a unique instance identifier

relative to I, e.g., by adding a replica count I_R , $0 \le I_R < R$. The pair (I, I_R) can then be used to sample t_r . To send the content object, it is split across packets, each of which carries the metadata as a header (plus the offset for the packet) and enqueued into the storage queue(s) of its local ISL 0 (and ISL 2) interface(s).

The originating satellite adjusts the initial value chosen for n based on its own position to ensure that the object is forwarded to the next orbital plane close to the equator: setting n > 0 reduces the number of hops before switching orbital planes; in this case, the object will not do a full circle through all of the initial orbit. The creator may retain a copy of the object after sending R replicas for later repair.

To determine if there is room for further insertions, satellites observe the object rotation time t_0 that represents the aggregate fill level of the overall storage system.¹

An object is deleted when its lifetime t_{ttl} expires, for which we may assume coarsely synchronized clocks across all satellites The originating satellite may also explicitly delete a content object: it simply stops forwarding any packets belonging to this object. With our strawman routing algorithm, this would deterministically clear the object from the orbital shell within t_0 as all packets pass through all satellites. Other forwarding algorithms may have to rely on the expiry time or craft explicit deletion packets ("anti-packets" [12]).

3.3 Error handling

Communication is subject to errors that lead to packet losses. Such errors include 1) bit errors on the laser link, 2) tracking/pointing errors when tracking the neighboring satellites, and 3) the reconfiguration time when connecting to a different neighboring satellite. While 1) may lead to individual packet losses, 2) could incur short loss bursts and 3) extended link unavailability and hence longer loss bursts or delays.

1) could be overcome by applying FEC (e.g., simple XOR, Reed-Solomon codes) mechanisms and ensure that all packets of an object can be recovered at each hop to avoid error accumulation. If content objects are small relative to the storage queue size, recovery could happen while the object is queued and thus not negatively affect periodicity. For 3), a simple approach is predicting when a reconfiguration of a satellite link is to occur and route to the next orbital plane one satellite earlier or later. The rerouting satellite needs to consider its own and its neighbors' queue capacity to not affect the overall stability of the system.

Concerning 2, assuming the above FEC mechanisms won't suffice to cope with an outage, a simple fallback mechanism could be used: if restoring a replica fails, the satellite in question could just drop all its packets and rely on the source node to re-instantiate the replica. For this, the creator monitors if still all R replicas of its objects circulate and recreates the missing ones if a gap in unique replica numbers is detected. This would just cause a temporary spike in periodicity and repair would happen within $O(t_0)$. Originators could also send content objects using rateless codes (e.g., fountain codes) for initial redundancy and add further encoding symbols in response to observed losses.

¹This somewhat coarsely resembles FDDI token ring networks that use a *target token rotation time* to determine the current utilization of the ring and thus if an attached station is allowed to send data [9].

4 INITIAL EVALUATION

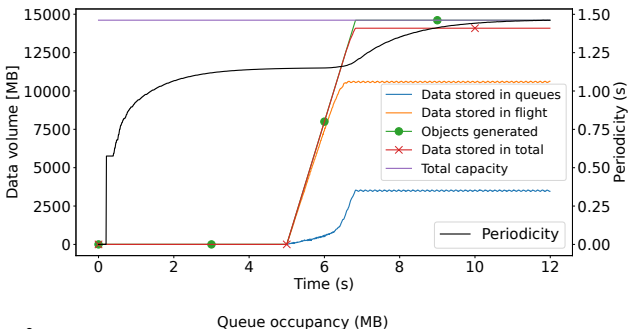
To understand how does the above strawman design works "in practice", we developed a custom simulator in Python that implements the connectivity pattern of fig. 3 and the forwarding algorithm of fig. 6. Objects are forwarded as messages and only processed by the receiver after they were received in full, for which a dedicated receive buffer is available. Once received, an object is moved to the next hop storage queue provided that there is enough space; otherwise it waits in the receive buffer. Objects sourced at a satellite are kept in a source queue and wait there until there is enough space in the next hop queue. Forwarding objects takes precedence over introducing new locally sourced ones. In our simulations, we introduce dedicated tokens (size: 1024 B), one per orbital plane, to continuously measure the rotation time. For our initial evaluation of the basic system properties, we consider only a period with stable satellite topology. Simulations operate in ticks of 1 ms and collect statistics every 10 ms.

We are interested in how the system stores incoming objects and how the rotation time evolves compared to our theoretical considerations. Therefore, we simulate the ramp-up phase from an initially empty system until its theoretical storage capacity is exhausted. We use a warmup time until all tokens have rotated once through the constellation so that each satellite can independently compute the rotation time. After the warmup, we start generating objects of fixed or variable size in fixed intervals (just one replica per object, $t_{ttl} = \infty$) at randomly chosen satellites (uniform distribution). We observe the data volume of the objects that are effectively stored in the system, the evolution of the rotation time (measured via our tokens), and the queue sizes across all satellites.

4.1 Basic operation

Fig. 7 shows a sample run for the Iridium constellation of 66 satellites $(N_p = 6 \text{ orbits}, N_o = 11 \text{ satellites}, a = 871 \text{ km})^2$ After a warmup time of 8 s, objects are generated in 1 ms intervals, the total data volume of data generated indicated by the green line. In the beginning, objects are usually sent immediately when they are sourced as the queues are mostly empty, shown by the steep slope of orange line representing data stored in flight, closely following the objects generated. This is confirmed by the curve for data stored in queues only growing gradually in the beginning. At around 6.5 s, an inflection point is reached and, statistically, all queues always contain data so that all the links are constantly busy and no more data can be stored in flight, so that further generated objects increase the share of data stored in queues. At around 7 s, the system is saturated and no further objects can be accepted. At this point, the theoretical system capacity (purple line at the top) is not fully reached, i.e., a fraction of objects never make it from the source queue into the system.

This effect is expected because sourcing new objects is distributed randomly across the satellites: since forwarding objects takes precedence, a newly sourced object can only enter the storage queue if there is room. Once a queue becomes full, it can only drain is there is less incoming than outgoing traffic. However, at a certain fill level,



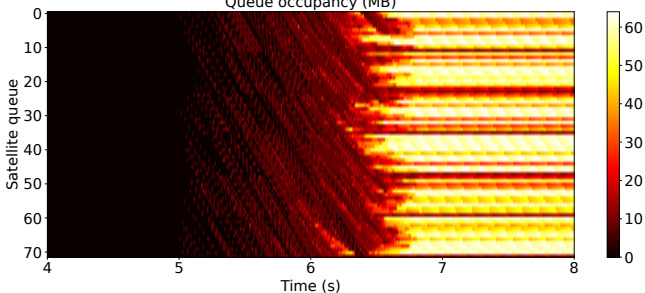


Figure 7: Evolution of storage utilization for $Q_S = 64 \, \text{MB}$ and $S = 8 \, \text{MB}$ in the simulated Iridium constellation: a) shows how much of the sent data is stored in queues vs. in flight as well as the evolution of the mean rotation time measured across all satellites (top); b) depicts the evolution of queue occupancy of the satellite queues used (bottom).

all satellites have developed standing queues (at the above inflection point) so that all links are constantly busy and queues cannot drain.

We illustrate this by looking at the queue occupancy across all satellite queues: the Northbound queues of all satellites (0–10, 12–22, ... in the plot) plus the Eastbound ones for cross-orbit connectivity (11, 23, 34, ...). Initially, only a few objects pass through the queues, which are partly filled and then emptied again. Between 6 and 7 s, we see queues grow so that standing queues develop and queue sizes largely stabilize. While there is still room in some queues to hold further objects, this space isn't available to objects sourced at other satellites. The remaining darker, i.e., less occupied, queues are the Eastbound ones because new objects contributing to queue buildup are only inserted into the Northbound ones.

4.2 Subtle Backpressure

To alleviate this statistical effect, the system needs to "move" space in the queues around to those satellites what have new objects waiting. While this could happen over time as objects expire, such an optimistic do-nothing-and-wait approach would only work proabilistically. Instead, we seek to actively make room. Since queues only drain if the incoming rate is less than the outgoing rate, we can apply some backpressure to ask the preceding satellite to reduce the outgoing rate. This must be done with care because: 1) any reduction in data rate immediately reduces the in-flight storage capacity. 2) Every satellite has a predecessor, all of which ultimately form a circle, so we must beware of cascading and oscillation effects.

²We use Iridium here because its constellation with just 66 satellites helps readability of the following graphs; result summaries for today's megaconstellations are included in Appendix B.

At a storage traffic rate of 80 Gbps for the ISLs, a rate change of 1% rate yields 100 MB/s and hence can assist shifting queue occupancy at short timescales. Based upon extensive simulations, we choose to limit rate adjustment $R_{adj} \in [0.0, 1.0]\%$. We define a simple feedback message sent to a neighbor satellite if the own send queue is full and (sourced) data is pending to ask the neighbor to reduce its traffic by R_{adj} . We compute R_{adj} , capped at 1%, from the space in the send queue of an ISL, the size of waiting locally sourced objects, and the ratio of the incoming to outgoging traffic rate so that the queue drains faster than it fills until there is enough room to hold the locally sourced objects. These control messages propagate into the opposite direction and hence do not interfere with data traffic, but they could also go into a priority queue to ensure transmissioin without delay.

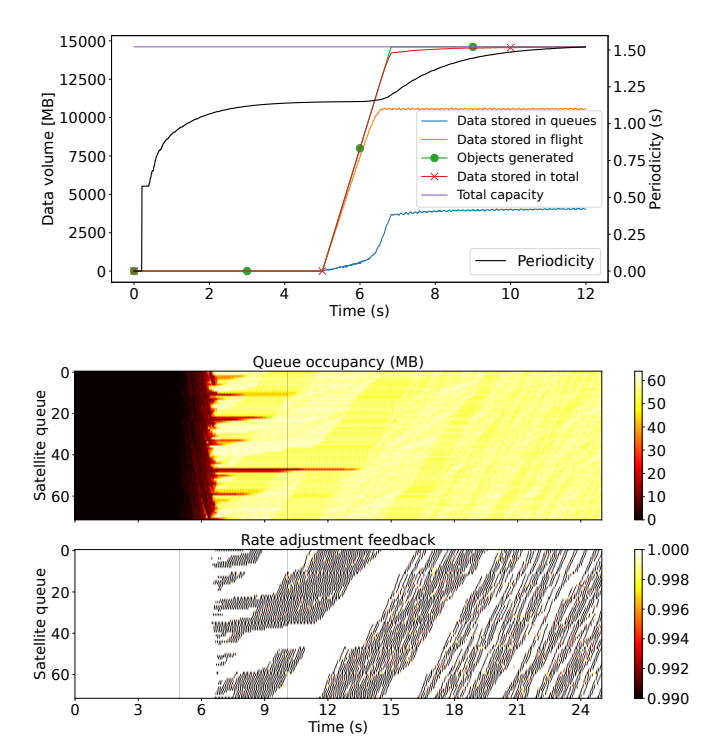


Figure 8: Applying a simple backpressure protocol helps utilizing the full storage capacity (top) and dissolve the standing queues (middle). The bottom plot shows where which backpressure is applied.

Fig. 8 depicts the effects of applying the simple backpressure protocol. The objects *stored in total* now reaches the *objects generated* (top) and the standing queues are dissolved (middle). The plot also shows the rate adjustments applied to each queue over time (bottom), indicating that the system enters and stays in a state of constant flux of minor rate adjustments. This is due to the communication latency between neighboring satellites that delays the effect of the rate adjustments: simulations without delays have shown the system to stabilize. We leave exploring proactive adjustment algorithms that can make up for the latency for future study.

The above figures show findings for the small Iridium topology to illustrate the observed effects. Appendix B also summarizes the results for the ten constellations also shown in fig. 5.

5 DISCUSSION AND CONCLUSION

In this paper, we take an unconventional approach to distributed data handling: we exploit the vast distances in space between satellites to store data "in flight" and have objects constantly rotate through all access locations so that requesting nodes just have to wait for them to pass by—rather than fixing the (replicated) storage locations and maintaining an index to find the data via a control plane. The availability of powerful ISLs in LEO satellite megaconstellations could provide a foundation for such design. While our strawman algorithm makes full use of ISLs within an orbital plane and largely spared those interconnecting different orbital planes, other configurations are conceivable, including mixing different shells to differentiate on latency and capacity needs.

But what to do with a modest amount of distributed storage capacity of some 40–80 GB at an access latency of <10s (or more with additional delay)? Anything requiring large volumes such as CDNs [4] would need different mechanisms but other interesting uses come to mind: One option is building a global user directory (a key-value store) with entries exclusively updated by their owners, e.g., along the lines of a *Minimal Global Broadcast* [10]: 128 B per user would just require 675 MB of storage and be hardly noticeable, leaving room for growth; extending this to today's 5.5 bn Internet users would require 670 GB and thus 512 MB storage queues. Another idea is using space as a backup for critical infrastructure data, such as the globale BGP routing tables: the 1.5 GB data (Sep 2024, from routeviews.org) would fit easily and need only a very small link capacity share.

While we explored storage queues of various sizes, an interesting case is an effectively queueless system for global broadcasting with memory: as shown in table 3, small content objects of a total volume of 7–100 GB could circulate once per 1–11 s. We may exploit these properties to efficiently distribute state synchronization messages in global consensus protocols where individual transactions are rather small. This may allow for a small high-priority traffic share f_s , in some cases, even LEDBAT-style scavenging traffic may suffice: both could be a start to explore this concept further.

REFERENCES

- J. Benet. 2014. IPFS Content Addressed, Versioned P2P File System. arXiv.org. http://arxiv.org/abs/1407.3561
- [2] Debopam Bhattacherjee, Simon Kassing, Melissa Licciardello, and Ankit Singla. 2020. In-orbit Computing: An Outlandish thought Experiment?. In Proceedings of the 19th ACM Workshop on Hot Topics in Networks (HotNets '20). https://doi.org/10.1145/3422604.3425937
- [3] Debopam Bhattacherjee and Ankit Singla. 2019. Network topology design at 27,000 km/hour. In Proceedings of the 15th International Conference on Emerging Networking Experiments And Technologies (CoNEXT '19). https://doi.org/10. 1145/3359989.3365407
- [4] Rohan Bose, Saeed Fadaei, Nitinder Mohan, Mohamed Kassem, Nishanth Sastry, and Jörg Ott. 2024. It's a bird? It's a plane? It's CDN!: Investigating Content Delivery Networks in the LEO Satellite Networks Era. In Proceedings of the 23rd ACM Workshop on Hot Topics in Networks (HotNets '24). https://doi.org/10.1145/3696348.3696879
- [5] Bradley Denby and Brandon Lucia. 2020. Orbital Edge Computing: Nanosatel-lite Constellations as a New Class of Computer System. In Proceedings of the Twenty-Fifth International Conference on Architectural Support for Programming Languages and Operating Systems (ASPLOS '20). 16 pages. https://doi.org/10.1145/3373376.3378473

- [6] Simon Kassing, Debopam Bhattacherjee, André Baptista Águas, Jens Eirik Saethre, and Ankit Singla. 2020. Exploring the "Internet from space" with Hypatia. In Proceedings of the ACM Internet Measurement Conference (IMC '20). https://doi.org/10.1145/3419394.3423635
- [7] Tobias Pfandzelter and David Bermbach. 2021. Edge (of the Earth) Replication: Optimizing Content Delivery in Large LEO Satellite Communication Networks. In 2021 IEEE/ACM 21st International Symposium on Cluster, Cloud and Internet Computing (CCGrid). https://doi.org/10.1109/CCGrid51090.2021.00066
- [8] Tobias Pfandzelter and David Bermbach. 2023. Edge Computing in Low-Earth Orbit – What Could Possibly Go Wrong?. In Proceedings of the the 1st ACM Workshop on LEO Networking and Communication 2023 (LEO-NET '23). https://doi.org/10.1145/3614204.3616106
- [9] F. Ross. 1986. FDDI A tutorial. IEEE Communications Magazine 24, 5 (1986). https://doi.org/10.1109/MCOM.1986.1093085
- [10] Christian Tschudin. 2023. Minimal Global Broadcast. Contribution to the IRTF DINRG meeting.
- [11] Ruolin Xing, Mengwei Xu, Ao Zhou, Qing Li, Yiran Zhang, Feng Qian, and Shangguang Wang. 2024. Deciphering the Enigma of Satellite Computing with COTS Devices: Measurement and Analysis. In Proceedings of the 30th Annual International Conference on Mobile Computing and Networking (ACM MobiCom '24). https://doi.org/10.1145/3636534.3649371
- [12] Xiaolan Zhang, Giovanni Neglia, Jim Kurose, and Don Towsley. 2007. Performance Modeling of Epidemic Routing. *Computer Networks* 51, 10 (2007). https://doi.org/10.1016/j.comnet.2006.11.028
- [13] Ruili Zhao, Yongyi Ran, Jiangtao Luo, and Shuangwu Chen. 2022. Towards Coverage-Aware Cooperative Video Caching in LEO Satellite Networks. In GLOBECOM 2022 - 2022 IEEE Global Communications Conference. https://doi.org/10.1109/GLOBECOM48099.2022.10001098

A NOTATION USED IN THIS PAPER

Table 1 summarizes the notation used in this paper.

Symbol	Explanation
r	Earth radius (≈ 6371 km)
a	sallite altitude above ground
d	distance between two consecutive satellites in the same orbital plane
d_p	distance between two adjacent orbital planes at the equator
$\hat{d_s}$	max distance between two satellites on adjacent orbital planes around the equator
N_o	number of satellite per orbital plane
N_p	number of orbital planes in a constellation
R_{ISL}	data rate of the ISL laser links
f_s	fraction of R_{ISL} allocated to storage traffic
Q_S	size of the storage queue
F_s	Data volume in flight between two satellites on the same orbit at rate $R_{ISL} \times f_S$
C_s	STorage capacity per satellite: $C_S = Q_S + F_S$
C _s C _p C _o	Storage capacity per orbital plane: $C_p = C_s \times N_o$
$\hat{C_o}$	Storage capacity of the orbital shell $C_O = C_p \times N_p$
K	number of replicas per content object
C_e	effective storage capacity of the orbital shell with K replicas: $C_e = C_O/K$
c	speed of light in vacuum: $c = 299,792.458 km/s$
t_f	processing delay per satellite: $t_f = 0.1 \mathrm{ms}$
t_q	queuing delay per satellite: $t_q = f_s \times Q_s / R_{ISL}$
t_p	propagation delay between consective satellites within an orbit: $t_q = d/c$
$\dot{t_s}$	propagation delay between satellites in adjacent orbits at distance d_s : $t_q = d_s/c$
t_o	rotation time of a single object through all satellites of an orbital shell
t_a	mean access time to one of K replicas of an object in a orbital shell
t_s	submission time of a newly created object to a satellite
t_e	time at which a newly created object enters the storage queue
t_w	waiting time between object creation and its entering the storage queue: $t_w = t_e - t_s$

Table 1: Overview of the symbols and notation

B DETAILED SIMULATION RESULTS

This appendix has further details on our simulations results for all the network topologies we investigated; those are summarized in table 2. As discussed above, the storage capacity of these megaconstellations is a function of the queue size per outgoing satellite link and the data in flight between any two satellites on the circular path through the orbital shell. The in-flight capacity obviously grows linearly with the number of orbits (plus marginally with the altitude) while the queue capacity grows linearly with the number of satellites; this also holds for the periodicity t_a of a data object.

Constellation	Altitude	#orbits	#sats/orbit	Inclination
S1: Starlink 1	550 km	72	22	53.0°
S2: Starlink 2	1110 km	32	50	53.8°
S3: Starlink 3	1110 km	8	50	74.0°
S4: Starlink 4	1275 km	5	75	81.0°
S5: Starlink 5	1325 km	6	75	70.0°
K1: Kuiper 1	630 km	34	34	51.9°
K2: Kuiper 2	630 km	36	36	43.0°
K3: Kuiper 3	590 km	28	28	33.0°
T1: Telesat 1	1015 km	27	13	98.98°
T2: Telesat 2	1325 km	40	33	50.88°
I: Iridium	871 km	6	11	86.4°

Table 2: LEO megaconstellation characteristics [6]

We carry out simulations using our custom simulator, written in Python, that simulates a short (stable) period in a +grid topology. We simulate different queue sizes $Q_s \in \{16, 32, 64, 128, 192, 256\}$ MB and explore constant objects sizes of $s \in \{1, 2, 4, 8, 16\}$ MB as well as objects sizes uniformly distributed in $s \in [1, 16]$ MB. We compute the maximum capacity C_O as per $\S 2.2$ of a (constellation, queue size) pair and then, after a warmup period (> t_a), fill the system up to 100% capacity, with new objects generated in 1 ms intervals at a randomly chosen satellite; objects do not expire. After capacity is reached, we run the simulation for another 10 s to determine if all objects are distributed across the storage queues.

We explore both the baseline operation (§4.1) and the simple back-pressure mechanism (§4.2). To characterize the system operation, we consider two metrics: 1) The object waiting time t_w is defined as the difference between the time t_s at which the object is created at (or: submitted to) the source queue of a satellite for storage and the time t_q at which the respective object leaves the source queue and enters the storage queue and thus is effectively stored in the syste: $t_w = t_q - t_s$. Recall that stored objects take precedence over newly generated ones so that a newly created object can only enter the system if the storage queue has enough space, hence, this is a measure for the agility of the system. 2) We count n_f how many objects (if any) were not accepted into the storage system (before the end of the simulation), i.e., $t_w = \infty$, dubbed (submission) failure.

We run each simulation with ten different random seeds and report the mean number of objects created, the mean number of failure n_f , and the maximum waiting time t_w . We show the results in tables 4–14. For each message size, the upper line of the row indicates the performance of the baseline operation (§4.1), whereas the lower line shows results with backpressure (§4.2).

Across almost all simulated configuration, we find that the simple backpressure algorithm can substantially reduce the number of object submission failures by shifting queue contents around. The exception is when the queue size equals the object size, $Q_s = s = 16 \, \mathrm{MB}$, in which case the message either all fit without backpressure or backpressure won't help. For the failures, note that n_f includes objects that were created close to the end of the simulation but could not be sent before the simulation ended—which may hold for some configurations with large queue sizes.

Const.			Per	iodicity	y (s)				St	orage	capac	ity (G	B)	
Q _s (MB)	-	16	32	64	128	192	256	-	16	32	64	128	192	256
Starlink 1	10.9	13.6	16.4	22.0	33.1	44.2	55.3	97	122	146	196	295	394	493
Starlink 2	5.3	8.1	10.8	16.3	27.2	38.2	49.2	47	72	97	147	247	347	447
Starlink 3	1.4	2.1	2.8	4.2	6.9	9.7	12.4	12	18	24	37	62	87	112
Starlink 4	1.0	1.6	2.3	3.5	6.1	8.6	11.2	7	13	19	31	54	78	101
Starlink 5	1.2	1.9	2.7	4.2	7.3	10.3	13.4	9	16	23	37	65	93	122
Kuiper 1	5.3	7.3	9.3	13.3	21.2	29.2	37.2	46	64	83	119	191	263	335
Kuiper 2	5.6	7.8	10.0	14.5	23.5	32.4	41.3	49	69	90	130	211	292	373
Kuiper 3	4.3	5.7	7.0	9.8	15.2	20.7	26.1	38	50	62	87	136	185	234
Telesat 1	4.4	5.0	5.7	6.9	9.5	12.0	14.5	39	44	50	60	82	104	126
Telesat 2	6.8	9.0	11.3	15.9	25.0	34.1	43.3	60	81	101	142	225	307	390
Iridium	1.1	1.2	1.3	1.5	2.0	2.5	3.0	8	9	10	12	17	21	25

Table 3: Periodicities and max storage capacities for different satellite constellations and queue sizes. These theoretical values do not consider the inter-orbit links and queues, while the simulations below do, which leads a systematically lower values in this table.

Q_s		16 MB			32 MB			64 MB			128 MB			192 MB			256 MB	
s (MB)	# obj	n_f	$\max t_w$	# obj	n_f	$\max t_w$	# obj	n_f	$\max t_w$	# obj	n_f	$\max t_w$	# obj	# fails	max tw	# obj	n_f	$\max t_w$
1	128404	11	0.533	154900	808	1.228	207892	2995	0.488	313876	7467	0.6	419860	11859	0.722	525844	15942	0.272
1	120404	0	0.018	134700	0	0.108	207092	0	0.24	313670	0	0.559	417000	0	4.475	323644	0	1.933
2	64202	7	11.196	77450	611	0.086	103946	2063	0.431	156938	4674	1.038	209930	7057	0.833	262922	9376	3.457
	04202	0	0.046	11430	0	0.942	103740	0	1.542	150756	0	4.202	207730	0	4.683	202722	0	5.949
4	32101	0	6.332	38725	543	1.358	51973	1592	0.297	78469	3279	1.025	104965	4714	0.748	131461	6038	1.047
4	32101	0	2.928	36723	0	6.23	31973	1	9.844	70409	3	12.312	104903	6	12.811	131401	26	17.982
8	16050	0	3.238	19362	368	1.992	25986	1157	0.225	39234	2260	0.528	52482	3152	2.092	65730	3975	0.313
	10030	0	3.238	19302	6	11.777	23900	16	10.943	37234	56	13.057	32462	105	15.135	03730	163	15.173
16	8025	671	1.305	9681	50	9.769	12993	511	0.249	19617	1216	0.193	26241	1792	0.144	32865	2294	0.122
10	8023	671	1.305	7001	8	10.83	12993	23	11.415	19017	66	12.292	20241	110	14.439	32003	176	16.095
1.16	15106	3	10.822	18223	2	9.089	24457	29	12.379	36926	94	15.378	49395	162	19.435	61864	234	21.841
1,10	15100	3	10.347	10223	0	10.259	24437	0	11.131	30920	1	11.571	+2393	4	13.195	01004	4	14.338

Table 4: Constellation starlink-1 storage properties

Q_s		16 MI	3		32 MB			64 MB			128 MB	3		192 MB			256 MB	
s (MB)	# obj	n_f	$\max t_w$	# obj	n_f	$\max t_w$	# obj	n_f	$\max t_w$	# obj	n_f	$\max t_w$	# obj	# fails	$\max t_w$	# obj	n_f	$\max t_w$
1	75496	0	0.0	101608	44	0.007	153832	732	0.027	258280	2831	0.439	362728	4979	0.26	467176	7037	0.041
1	73490	0	0.0	101008	0	0.035	133632	0	0.052	236260	0	0.099	302728	0	0.15	40/1/0	0	0.24
2	37748	0	0.0	50804	84	0.062	76916	773	0.392	129140	2363	0.13	181364	3831	0.354	233588	5218	0.334
1 -	37770	0	0.0	30004	0	0.087	70710	0	0.137	127170	0	0.748	101304	0	1.236	233366	0	4.043
4	18874	0	0.019	25402	124	1.314	38458	828	0.147	64570	2045	0.122	90682	3057	0.156	116794	3988	0.238
	10074	0	0.019	23402	0	0.544	30430	0	3.013	04370	0	4.082	90002	0	8.987	110/54	0	11.35
8	9437	0	0.204	12701	98	10.16	19229	705	0.365	32285	1606	0.166	45341	2296	1.677	58397	2916	1.311
	7431	0	0.204	12/01	0	1.36	1/22/	0	6.592	32203	2	13.329	73371	9	14.506	36371	22	14.142
16	4718	0	2.186	6350	0	8.011	9614	334	0.165	16142	943	0.057	22670	1420	0.048	29198	1809	0.134
10	7/10	0	2.186	0550	0	1.163	7014	0	9.684	10142	9	12.444	22070	34	13.927	27170	69	14.879
1.16	8881	0	0.497	11953	0	4.23	18097	16	12.333	30385	61	16.095	42673	109	16.986	54961	167	17.941
1,10	0001	0	0.579	11755	0	2.025	10077	0	2.848	30303	0	8.722	42073	0	12.553	34701	1	12.428

Table 5: Constellation starlink-2 storage properties

Q_s		16 MI	В		32 MI	В		64 MF	3		128 M	В		192 MB			256 MB	
s (MB)	# obj	n_f	$\max t_w$	# obj	# fails	$\max t_w$	# obj	n_f	$\max t_w$									
1	19944	0	0.0	26472	12	0.005	39528	188	0.254	65640	687	0.076	91752	1220	0.272	117864	1737	0.091
1	19944	0	0.0	20472	0	0.02	39326	0	0.062	03040	0	0.519	91/32	0	1.66	11/604	0	2.787
2	9972	0	0.001	13236	20	0.012	19764	207	0.393	32820	591	0.065	45876	961	0.083	58932	1285	0.079
	9912	0	0.001	13230	0	0.099	19704	0	1.287	32020	0	1.959	43070	0	3.874	36932	0	4.199
4	4986	0	0.109	6618	35	0.012	9882	207	0.152	16410	510	0.778	22938	762	0.147	29466	995	0.086
1 7	4700	0	0.07	0016	0	0.647	7002	0	2.323	10410	0	6.031	22936	0	8.656	23400	0	11.956
8	2493	0	0.37	3309	32	10.598	4941	179	0.145	8205	409	0.137	11469	578	0.124	14733	732	0.146
0	2493	0	0.37	3309	0	4.528	4241	0	8.05	0203	3	11.544	11409	6	11.421	14733	25	11.651
16	1246	0	1.905	1654	0	3.018	2470	89	6.98	4102	238	3.001	5734	353	1.788	7366	458	2.304
10	1240	0	1.905	1034	0	2.881	24/0	2	9.631	4102	7	10.912	3734	19	11.06	/300	26	11.81
1,16	2346	0	0.403	3114	0	1.266	4650	4	8.672	7722	21	10.246	10794	34	11.29	13866	47	10.78
1,10	2340	0	0.422	3114	0	1.65	4030	0	3.191	1122	0	10.616	10/94	0	10.2	13800	1	11.527

Table 6: Constellation starlink-3 storage properties

Q_s		16 MI	3		32 M	3		64 MF	3		128 M	В		192 MB			256 MB	
s (MB)	# obj	n_f	$\max t_w$	# obj	n_f	$\max t_w$	# obj	n_f	$\max t_w$	# obj	n_f	max tw	# obj	# fails	$\max t_w$	# obj	n_f	max tw
1	15149	0	0.0	21229	9	0.033	33389	144	0.09	57709	570	0.07	82029	983	0.129	106349	1366	0.046
1	13149	0	0.0	21229	0	0.005	33369	0	0.066	31109	0	0.174	02029	0	1.257	100549	0	2.124
2	7574	0	0.0	10614	21	0.008	16694	170	6.248	28854	503	2.388	41014	819	4.726	53174	1094	8.658
	1314	0	0.0	10014	0	0.123	10074	0	0.588	20034	0	1.522	71017	0	3.653	33174	0	4.55
4	3787	0	0.009	5307	29	0.114	8347	185	0.105	14427	444	0.075	20507	665	0.12	26587	866	0.136
	3707	0	0.006	3307	0	0.495	0547	0	2.421	17727	0	4.679	20307	0	9.094	20307	0	9.9
8	1893	0	0.096	2653	26	0.299	4173	159	0.161	7213	365	0.121	10253	512	0.124	13293	646	0.111
	1075	0	0.096	2033	0	2.465	4173	0	5.749	7213	0	10.021	10233	4	12.838	13273	15	12.737
16	946	0	0.825	1326	0	1.928	2086	80	0.111	3606	211	0.291	5126	316	0.194	6646	410	0.231
10) 940	0	0.825	1320	0	1.283	2000	0	10.757	3000	4	10.71	3120	7	11.577	0040	22	11.645
1,16	1782	0	0.239	2497	0	0.573	3928	4	10.001	6789	17	10.374	9650	28	11.603	12511	44	12.708
1,10	1762	0	0.258	<u>∠</u> +91	0	3.875	3926	0	2.615	0/09	0	9.551	7030	0	10.405	12311	0	10.16

Table 7: Constellation starlink-4 storage properties

Q_s		16 MI	3		32 M	В		64 ME	3		128 M	В		192 MB			256 MB	
s (MB)	# obj	n_f	$\max t_w$	# obj	# fails	$\max t_w$	# obj	n_f	$\max t_w$									
1	17992	0	0.0	25288	11	0.145	39880	185	0.081	69064	718	0.105	98248	1259	0.12	127432	1793	0.101
'	1/992	0	0.0	23200	0	0.022	37000	0	0.037	09004	0	0.165	70240	0	1.609	127432	0	2.928
2	8996	0	0.0	12644	26	0.537	19940	226	0.321	34532	643	0.441	49124	1028	0.49	63716	1361	0.498
2	0990	0	0.0	12044	0	0.098	17740	0	0.586	34332	0	2.246	47124	0	4.524	03/10	0	6.295
4	4498	0	0.016	6322	40	0.241	9970	230	0.564	17266	563	1.04	24562	830	0.974	31858	1043	0.985
+	4470	0	0.016	0322	0	0.651	9910	0	4.198	17200	0	6.622	24302	1	11.755	31030	2	12.347
8	2249	0	0.14	3161	33	10.318	4985	197	0.149	8633	446	0.119	12281	635	0.648	15929	806	0.163
"	2249	0	0.14	3101	0	6.01	4703	0	5.081	8033	2	10.823	12201	5	12.223	13929	17	13.011
16	1124	0	1.151	1580	0	2.422	2492	96	0.137	4316	261	0.085	6140	388	0.039	7964	504	0.04
10	1124	0	1.151	1360	0	2.39	2492	0	10.351	4310	5	10.82	0140	11	11.45	7704	33	11.646
1,16	2116	0	0.272	2975	0	7.671	4691	4	10.511	8125	17	10.724	11558	36	12.543	14992	52	11.513
1,10	2110	0	0.302	2913	0	0.787	4071	0	2.962	0123	0	6.426	11336	0	9.036	14772	0	10.736

Table 8: Constellation starlink-5 storage properties

Q_s		16 MI	3		32 MI	3		64 MB			128 MB			192 MB			256 MB	
s (MB)	# obj	n_f	$\max t_w$	# obj	n_f	max tw	# obj	n_f	max tw	# obj	n_f	$\max t_w$	# obj	# fails	$\max t_w$	# obj	n_f	$\max t_w$
1	68111	0	0.001 0.001	87151	136 0	0.133 0.069	125231	1036 0	0.802 0.137	201391	3165 0	5.505 0.343	277551	5217 0	0.167 0.463	353711	7264 0	1.031 0.413
2	34055	0	0.004 0.004	43575	157 0	0.059 0.097	62615	869 0	0.05 0.705	100695	2351 0	1.378 1.99	138775	3662 0	3.248 4.836	176855	4892 0	1.984 7.375
4	17027	0	0.273 0.036	21787	186 0	0.972 0.845	31307	781 0	0.291 2.657	50347	1742 0	1.074 7.666	69387	2629 0	0.803 10.843	88427	3408 0	1.127 12.662
8	8513	0	1.116 1.116	10893	142 0	0.969 5.928	15653	626 1	0.713 10.424	25173	1333	2.242 12.377	34693	1872 18	1.579 13.096	44213	2371 57	0.938 15.127
16	4256	87 87	5.876 5.876	5446	2 0	10.086 6.231	7826	288 4	0.117 10.337	12586	762 17	0.081 12.029	17346	1133 45	0.892 13.427	22106	1453 80	0.274 14.21
1,16	8013	0	2.376 1.978	10253	0	8.424 4.02	14733	16 0	10.871 9.95	23693	51 0	11.527 10.557	32653	97 1	14.55 11.268	41613	144 2	14.534 11.996

Table 9: Constellation kuiper-1 storage properties

Q_s		16 MI	В		32 MI	3		64 MB			128 MB			192 MB			256 MB	
s (MB)	# obj	n_f	max t _w	# obj	n_f	$\max t_w$	# obj	n_f	$\max t_w$	# obj	n_f	max t _w	# obj	# fails	max tw	# obj	n_f	max t _w
1	73186	0	0.0	94498	22	0.003	137122	541	0.061	222370	2346	0.096	307618	4423	0.175	392866	6506	0.4
1	/3100	0	0.0	94496	0	0.012	13/122	0	0.092	222310	0	0.104	30/018	0	0.189	392000	0	0.302
2	36593	0	0.0	47249	60	0.033	68561	635	2.293	111185	1988	2.814	153809	3264	1.881	196433	4547	1.557
	30393	0	0.0	41249	0	0.058	06501	0	0.216	111103	0	1.11	133609	0	2.78	170433	0	3.182
4	18296	0	0.022	23624	88	0.181	34280	638	0.408	55592	1658	0.132	76904	2569	0.234	98216	3386	0.862
7	10290	0	0.022	23024	0	0.241	34200	0	2.005	33392	0	3.775	70904	0	7.094	70210	0	10.098
8	9148	0	0.205	11812	72	2.383	17140	556	2.13	27796	1288	2.048	38452	1931	0.951	49108	2463	2.141
	7170	0	0.205	11012	0	1.134	17140	0	6.866	21170	1	11.237	30432	6	14.895	47100	14	15.543
16	4574	0	7.308	5906	0	5.347	8570	268	1.432	13898	769	0.074	19226	1175	1.203	24554	1509	0.325
10	75/7	0	7.308	3700	0	3.118	0570	0	9.897	13070	8	11.545	17220	18	13.297	24334	52	14.913
1,16	8610	0	0.658	11117	0	3.83	16132	13	12.355	26161	51	16.913	36190	100	16.26	46219	146	19.686
1,10	0010	0	0.757	1111/	0	0.373	10132	0	4.421	20101	0	9.127	30190	0	12.369	70219	0	16.164

Table 10: Constellation kuiper-2 storage properties

Q_s		16 MI	В		32 MI	В		64 MI	3		128 MB			192 MB			256 MB	
s (MB)	# obj	n_f	max tw	# obj	n_f	$\max t_w$	# obj	n_f	$\max t_w$	# obj	n_f	$\max t_w$	# obj	# fails	$\max t_w$	# obj	n_f	$\max t_w$
1	53419	0	0.0	66411	47	0.01	92395	564	0.058	144363	2014	0.112	196331	3564	0.13	248299	5088	0.173
1 1	33417	0	0.0	00411	0	0.026	72373	0	0.114	144505	0	0.265	170331	0	0.479	240277	0	0.924
2	26709	0	0.002	33205	77	0.047	46197	522	2.743	72181	1505	11.831	98165	2468	2.928	124149	3351	2.75
	20709	0	0.002	33203	0	0.088	40197	0	1.244	72101	0	2.537	76103	0	3.615	124149	0	7.208
4	13354	0	0.357	16602	95	0.111	23098	495	0.113	36090	1189	0.12	49082	1789	0.123	62074	2371	0.124
+	13334	0	0.053	10002	0	1.277	23096	0	3.074	30090	0	4.948	49002	0	10.989	02074	0	10.887
8	6677	0	1.178	8301	79	5.654	11549	401	0.12	18045	893	0.16	24541	1294	0.172	31037	1658	0.124
0	0077	0	1.178	0301	0	5.281	11349	0	10.613	10043	3	12.983	24341	14	11.997	31037	29	13.205
16	3338	87	3.623	4150	0	8.034	5774	189	4.691	9022	507	2.213	12270	768	4.833	15518	998	0.164
10	3336	87	3.623	4130	0	4.083	3114	2	10.918	9022	8	11.944	12270	25	12.034	13316	51	13.175
1,16	6284	0	1.354	7813	0	4.359	10870	12	10.241	16983	42	12.143	23097	70	13.479	29211	101	13.373
1,10	0204	0	1.669	7013	0	3.433	100/0	0	8.42	10903	0	10.922	23097	1	11.885	29211	1	13.938

Table 11: Constellation kuiper-3 storage properties

Q_s		16 ME	3		32 MI	3		64 MB			128 MI	3		192 MB			256 MB	
s (MB)	# obj	n_f	$\max t_w$	# obj	n_f	$\max t_w$	# obj	n_f	$\max t_w$	# obj	n_f	$\max t_w$	# obj	# fails	$\max t_w$	# obj	n_f	$\max t_w$
1	47635	70	0.611	53683	436	0.25	65779	1235	0.788	89971	2826	0.247	114163	4416	2.583	138355	6002	0.397
1	4/033	0	0.778	33063	0	0.928	03119	0	1.304	099/1	0	2.802	114103	0	3.425	136333	0	4.091
2	23817	48	1.764	26841	281	0.427	32889	724	0.175	44985	1582	0.406	57081	2398	0.169	69177	3197	0.14
2	23017	0	1.601	20041	0	2.411	32009	0	3.143	44703	0	4.982	37001	0	6.171	09177	0	9.563
4	11908	2	9.356	13420	214	0.358	16444	490	0.903	22492	986	0.615	28540	1429	0.791	34588	1853	1.014
*	11900	0	9.255	13420	1	10.498	10444	4	10.889	22492	16	11.746	20340	31	12.878	34300	48	14.381
8	5954	0	6.67	6710	134	0.937	8222	334	0.143	11246	626	0.123	14270	893	0.12	17294	1122	0.117
0	3934	0	6.67	0/10	18	10.623	0222	30	11.492	11240	52	12.165	14270	71	12.535	1/294	88	13.375
16	2977	364	0.914	3355	32	10.486	4111	161	2.42	5623	339	1.534	7135	481	0.262	8647	621	0.418
10	2911	364	0.914	3333	11	10.956	4111	22	11.156	3023	43	11.412	/133	57	11.587	0047	79	10.97
1,16	5604	14	10.225	6315	1	5.46	7738	11	10.671	10584	35	10.687	13431	57	11.322	16277	81	11.932
1,10	3004	5	10.547	0313	0	10.45	1136	1	7.98	10304	2	10.473	13431	2	11.315	10277	5	12.608

Table 12: Constellation telesat-1 storage properties

Q_s	16 MB			32 MB			64 MB			128 MB			192 MB			256 MB		
s (MB)	# obj	n_f	$\max t_w$	# obj	n_f	$\max t_w$	# obj	n_f	$\max t_w$	# obj	n_f	$\max t_w$	# obj	# fails	max tw	# obj	n_f	$\max t_w$
1 8	84993	420	0.303	106753	1771	0.105	150273	3794	0.074	237313	7003	0.292	324353	9887	0.563	411393	12600	0.118
	07/73	0	0.466		0	2.54		0	7.201		0	9.045		0	10.067		1	11.593
2	42496	207	0.69	53376	1100	3.095	75136	2369	0.169	118656	4357	2.191	162176	6059	0.346	205696	7594	8.992
	42490	0	8.017		0	5.519		0	7.589		3	12.299		3	12.848		20	14.907
4	21248	101	10.049	26688	797	1.052	37568	1687	1.059	59328	2943	0.563	81088	4005	0.657	102848	4950	2.024
		4	10.802		11	10.815		30	11.406		66	14.125		105	15.53		164	15.636
8	10624	5	10.798	13344	498	2.255	18784	1127	0.865	29664	1983	1.539	40544	2643	0.727	51424	3230	0.57
		5	10.798		58	11.166		93	12.009		147	12.83		195	15.739		244	15.329
16	5312	543	1.108	6672	101	9.683	9392	513	0.208	14832	1075	0.142	20272	1506	0.107	25712	1868	0.095
		543	1.108		26	10.58	9392	45	12.382		91	12.659		134	13.95		192	15.031
1,16	9999	14	9.94	12559	6	10.812	17679	32	12.465	27919	87	14.808	38159	142	17.377	48399	193	18.219
		4	9.728		1	10.203		1	10.41		2	11.058		3	14.005		7	14.779

Table 13: Constellation telesat-2 storage properties

Q_s	16 MB			32 MB			64 MB			128 MB			192 MB			256 MB		
s (MB)	# obj	n_f	$\max t_w$	# obj	n_f	$\max t_w$	# obj	n_f	$\max t_w$	# obj	n_f	$\max t_w$	# obj	# fails	$\max t_w$	# obj	n_f	$\max t_w$
1	11155	5	4.135	12307	54	0.135	14611	187	0.15	19219	511	0.262	23827	861	0.286	28435	1221	0.223
		0	0.489		0	0.976		0	1.508		0	2.721		0	3.49		0	4.514
2	5577	0	1.831	6153	50	0.021	7305	137	0.551	9609	313	0.324	11913	491	0.21	14217	659	0.262
		0	1.154		0	1.506		0	2.478		0	3.403		0	4.693		0	5.652
4	2788	0	1.178	3076	40	0.127	3652	91	0.16	4804	183	1.318	5956	275	0.563	7108	362	0.959
		0	0.986		0	3.265		0	6.276		0	9.585		0	10.046		0	10.273
8	1394	0	1.327	1538	29	0.649	1826	63	0.077	2402	125	0.134	2978	179	0.045	3554	228	0.038
		0	1.327		0	9.236		1	10.084		2	10.774		7	10.157		14	10.56
16	697	82	0.329	769	4	2.877	913	30	0.156	1201	63	2.604	1489	92	2.183	1777	122	1.645
		82	0.329		0	3.972		1	9.864		3	10.883		6	10.654		12	10.31
1,16	1312	3	9.931	1447	0	6.407	1718	2	8.868	2261	7	10.799	2803	11	10.359	3345	16	10.211
		1	7.756	144/	0	1.336		0	6.362		0	7.903		0	10.248		1	10.699

Table 14: Constellation iridium storage properties